WHAT A DIFFERENCE HYPERTENSION MAKES: THE ADVENTITIA HANDS OFF TO PVAT FOR EXTRACELLULAR MATRIX REMODELING AS BLOOD PRESSURE RISES IN THE HIGH FAT FED DAHL SS RAT

By

Caitlin Wilson

A THESIS

Submitted to
Michigan State University
in partial fulfillment of the requirements
for the degree of

Laboratory Research in Pharmacology and Toxicology – Master of Science

2023

ABSTRACT

Tunica media extracellular matrix (ECM) remodeling is well understood to occur in response to elevated blood pressure, unlike the remodeling of other tunicae. We hypothesize that perivascular adipose tissue (PVAT) is responsive to hypertension and remodels as a protective measure. The adventitia and PVAT of the thoracic aorta were used in measuring ECM genes from 5 pairs of Dahl SS male rats on 8 or 24 weeks of feeding from weaning on a control (10% Kcal fat) or high fat (HF; 60%) diet. A PCR array of ECM genes was performed with cDNA from adventitia and PVAT after 8 and 24 weeks. A gene regulatory network of the differentially expressed genes (DEGs) (HF 2-fold > Con) was created using Cytoscape. After 8 weeks, 29 adventitia but 0 PVAT DEGs were found. By contrast, at 24 weeks, PVAT possessed 47 DEGs while adventitia had 3. Top DEGs at 8 weeks in adventitia were thrombospondin 1 and collagen 8a1. At 24 weeks, thrombospondin 1 was also a top DEG in PVAT. The transcription factor *Adarb1* was identified as a regulator of DEGs in 8 week adventitia and 24 week PVAT. These data support that PVAT responds biologically once blood pressure is elevated.

TABLE OF CONTENTS

INTRODUCTION

Elevated blood pressure (hypertension) puts arteries to the test. When exposed to a higher-than-normal blood pressure, the cells of the artery rearrange themselves; lay down more collagen to strengthen the vessel wall (fibrosis); and increase cell number (hyperplasia) (Humphrey, 2021). This process, described as remodeling of the artery, is best recognized in two tunica of the vessel, the tunica media and to a lesser extent the tunica adventitia (Majesky & Weiser-Evans, 2022, Majesky et al., 2012, Michel et al., 2021, McGrath et al., 2005, Siow & Churchman, 2007, Coen et al., 2011). Remodeling is also recognized in the many species in which the vasculature has been studied, from the mouse to the human. Missing from this is the consideration that the tunica adiposa, equivalent to the perivascular adipose tissue (PVAT), may also remodel in hypertension.

PVAT is best recognized for its ability to produce anticontractile substances (Xia & Li, 2017, Gollasch, 2017). PVAT responds to hypertension/cardiovascular disease with a loss of anticontractile function due to a lower production or effectiveness of substances that reduce contraction. These include nitric oxide, hydrogen sulfide, and adiponectin to name a few. This knowledge is important but is limited in consideration of the overall functions of PVAT. We have a long-term hypothesis that PVAT has the potential to mechanosense and mechanorespond. One could argue that the loss of anticontractile function in the face of hypertension is just one such example of mechanosensing and responding to a change in pressure. Presently, we turn to a different response of PVAT, that of extracellular matrix (ECM) remodeling in the face of hypertension.

The media (Humphrey, 2021) and, to some extent, the adventitia (Majesky & Weiser-Evans, 2022, Majesky et al., 2012, Michel et al., 2021, McGrath et al., 2005, Siow & Churchman, 2007, Coen et al., 2011) remodel with/after development of an elevated blood pressure with elevation in ECM proteins that ultimately increase fibrosis of the artery. Here, we test the specific hypothesis that PVAT remodels its extracellular matrix to become more fibrotic, as measured by changes in genes recognized to play a role in this process. In this study, we compare the PVAT to the adventitia directly. This is because the adventitia serves as the basement for PVAT, its closest neighbor. Also, the adventitia is collagen rich, while PVAT is comparatively collagen poor in the normal state (Watts et al., 2021). The model used is the Dahl SS male rat made hypertensive by being fed a high fat (HF) diet from weaning (Beyer et al.,

2012, Fernandes, et al., 2018). The thoracic aorta, which is exposed to the highest blood pressures in the body, is the arterial model. Use of this specific artery provided three benefits. First, the PVAT of this tissue is discrete to this artery; it is not shared with a vein. Second, the thoracic aorta is large enough such that the adventitia can be dissected off from the media. Third and finally, the individual tunicas of one thoracic aortic media and adventitia provide sufficient RNA such that a full plate of ECM genes can be run for each tissue. This allows for a powerful comparison between adventitia and PVAT within one animal.

MATERIALS AND METHODS

Animals and Diet

Dahl SS male rats, just weaned (3-4 weeks of age), were purchased from Charles River Laboratories (RRID:RGD_2308886; Kingston, NY, USA). Once received at MSU, rats were randomized to Control diet or HF diet and fed for either 8 (N=5 pairs) or 24 weeks (N= 5 pairs). A total of twenty (20) rats were used in this study. The experiments that result from animals on diet at these two time points were carried out at independent times. Rats are given a unique group number and ear clipped to distinguish one from another. Animals were group housed (2/3 per cage dedicated to one diet) on a 12-hour light/dark cycle at 22–25°C room temperature. The animals were housed with Heat Treated Aspen Hardwood Laboratory Bedding (Northeastern Products Corp., Warrensburg, NY USA). The Control diet was 10% kCal fat (lard) and 0.2% Na (Diet D12450J, Research Diets, New Brunswick, NJ, USA) while the High Fat (HF) diet was 60% kCal high fat (lard) and 0.3% Na (Diet D12492). Diets were well labelled in a freezer in the same room housing experimental rats. Food and water were available *ad libitum.* MSU animal care staff and study staff worked together to ensure that food was fresh and feeding of a specific diet was not interrupted during the course of experiments. Procedures using animals complied with National Institutes of Health "Guide for the Care and Use of Laboratory Animals" (2011). Procedures used were approved by the MSU Institutional Animal Care and Use Committee (PROTO202000009). Finally, this study was conducted with "Animal Research: Reporting of In Vivo Experiments "(ARRIVE) guidelines (essential 10 and recommended) in mind.

Sphygmomanometry

Blood pressure measurements of rats were made by sphygmomanometry in conscious, restrained and warmed (~ 37°C for 3-5 minutes) rats. The animal was placed in a restraint device designed to maintain body temperature and keep the animal calm. The entire measurement process was automated *via* a computer program that controls the apparatus (CODA High Throughput system, Kent Scientific, Torrington, CT, USA). The tail-cuff was inflated 15 times (to a pressure of ~ 250 mmHg with a slow deflation over a period of ~ 15 seconds) with thirty-second intervals between inflations. Blood pressure was obtained during each inflation cycle by a volume pressure recording sensor; the final reading was the average of ten inflations. While this system non-invasively measures systolic, diastolic, and mean arterial pressure, we report

only mean arterial pressure. Once the measures were done, animals were returned to their home cage. This measure was made at least once during the time on diet and the day before animals were taken for experimentation.

Dissection

Rats were given pentobarbital as a deep anesthetic (80 mg kg^{-1}, ip). A bilateral pneumothorax was created prior to vessel dissection from the rat. The thoracic aorta was dissected from the aortic arch to the diaphragm. Tissue dissection took place under a stereomicroscope and in a Silastic®-coated dish filled with physiological salt solution (PSS) containing [mM: NaCl 130; KCl 4.7; KH_2PO_4 1.18; $MgSO_4 \cdot 7H_2O$ 1.17; $NaHCO_3$ 14.8; dextrose 5.5; $CaNa_2EDTA$ 0.03, $CaCl_2$ 1.6 (pH 7.2)]. The whole aorta was threaded onto a wire mounted in a black silastic-filled dish. One small ring (2 mm wide) containing all arterial tunica was dissected off for histology (below). The wire was then secured to the silastic and all PVAT dissected off from the whole of the mounted aorta; this became the PVAT sample for the RT^2 Profiler Arrays. The aorta was then removed from the wire, cut longitudinally and pinned lumen-side down. The adventitia was scored with a scalpel and gently teased off the media. This became the adventitia sample for the RT^2 Profiler Arrays.

Histology

Immediately upon dissection, the 2 mm rings of thoracic aorta were formalin (10%)-fixed and paraffin embedded by MSU Investigative Histopathology. Sections (8 micron thick) were cut and tissues stained standardly with Masson Trichrome Stain. Sections were photographed on a Nikon TE2000 inverted microscope using a Nikon Digital Sight DS-Qil camera and Nikon NIS Elements BR 4.6 software. Settings were determined using tissue without stain as a negative control and were used consistently across all images.

RNA Isolation, Quantification and Purity

Adventitia (9 - 34 mg from the 5 aortae) or thoracic aortic PVAT (48 - 93 mg) was homogenized in 2 mL Beadruptor tubes with 1.4 mm ceramic bead media (catalog # 19-645-3, Omni International, Kennesaw, GA, USA) and 900 mL Qiazol Lysis Reagent (from Universal Mini Kit) in an Omni Beadruptor (Omni International; speed = 5.65 m/s, time = 30 seconds, cycles = 2). Following disruption, RNA was isolated with the RNeasy Plus Universal Mini Kit (catalog # 73404, Qiagen, Germantown, MD, USA) according to manufacturer's recommended protocol. RNA concentration and purity were determined using a Nanodrop 2000c (Thermo Scientific, Waltham, MA, USA).

cDNA Preparation

The RT^2 First Strand Kit (catalog # 330421, Qiagen, Germantown, MD, USA) was used according to manufacturer's recommended protocol to reverse transcribe 0.5 mg RNA into cDNA in a SimpliAmp thermal cycler (Applied Biosystems, Waltham, MA, USA).

Extracellular Matrix and Cell Adhesion RT^2 Profiler Arrays

A single array plate (RT^2 Profiler™ PCR Array Rat Extracellular Matrix & Adhesion Molecules; GeneGlobe ID - PARN-013Z, Qiagen, Germantown, MD, USA) was used for comparison of extracellular matrix genes between each tissue and types of tissue. Adventitia and PVAT samples for each animal were run on individual plates; these plates were run on the same day. In this way, the adventitia and PVAT of the same aorta could be best compared. The PCR conditions were as follows (run on Applied Biosystems Quant Studio 7 Flex system connected to a Dell Optiplex XE2 computer:

1 cycle of 95°C 10 minutes;

40 cycles of 95°C 15 seconds;

60°C 1 minute

RT^2 SYBR Green Master Mix (catalog # 330623, Qiagen, Germantown, MD, USA) was used for all SuperArray plates. As stated in the RT^2 Profiler PCR Array Handbook, the threshold value is determined when C_T^{PPC} is 20 ± 2. All plates in this study were set to the same value of 0.16. Data were exported (described below).

Array Analysis

The RT^2 Profiler Array uses a Microsoft Excel-based file that allows for import of C_T values from the real-time PCR machine. Data were gathered in separate Excel sheets for each of the following four comparison: 8 week Adventitia HF *vs* Control; 8 week PVAT HF *vs* Control; 24 week Adventitia HF *vs* Control; and 24 week PVAT HF *vs C*ontrol. In each sheet, C_T values were compared to the average of five (5) different reference genes: b-actin (*Actb*), beta-2-microglobulin (*B2M*), hypoxanthine phosphoribosyltransferase 1 (*Hprt1*), lactate dehydrogenase A (*Ldha*) and Ribosomal protein, large, P1 (*Rplp1*). The 2^{-DCT} were calculated for the gene of interest where DC_T is [C_T value of the gene of interest – C_T value of averaged housekeeping gene]. From this, the fold change of HF/control was calculated. These are the values reported in **Supplemental Table 1**. A fold change of 2.00 or above was considered biologically meaningful. Statistically, the p values were calculated based on a Student's t-test of the replicate 2^{-DCT} values

for each gene in the Control group and Treatment (HF) groups.

Generation of Volcano Plots of Differential Gene Expression at 8 and 24 Weeks on Diet

Volcano plots were used to highlight the upregulated and downregulated genes in each tissue. Plots were generated using the RT^2 Profiler Array analysis Excel document. The plots were modified to highlight the gene names of the top differentially expressed genes in each tissue and timepoint, denoted by black dots.

Construction of Color Plots to Visualize Fold Change

The Cytoscape application (Shannon et al., 2003) was leveraged to visualize the genes that were upregulated with a fold-change (FC) ≥ 2 with a color-intensity plot. A fold-change of 2.00 is represented by the lightest color, and as the fold-change increases the color darkens in turn. These values were used to create a quantitative Venn diagram of Differentially Expressed Genes (DEGs) at 24 weeks where the shape fill represents PVAT gene FC, and the shape outline is indicative of adventitia gene FC.

Construction of Gene Regulatory Network

The Cytoscape plugin iRegulon was employed to understand the regulatory interactions among the DEGs within PVAT and adventitia at week 8 and 24 on HF *vs* Control diet through the construction of a gene regulatory network. iRegulon predicts transcription factors (TFs) involved in regulating co-expressed gene sets through the ranking of enriched motifs using position weight matrices (PWM) (Janky et al., 2014). Mus musculus was used in analysis as species for both analyses as there was no rat species offered in the program. The minimum identity between orthologous genes was set to 0.05, while the maximum false discovery rate (FDR) on motif similarity was defined as 0.001. The gene regulatory network was constructed using a threshold of >4 normalized enrichment score (NES) to select TFs for analysis in both tissues at 8 and 24 weeks.

Immunohistochemistry protocol for thrombospondin1 expression

Sections made from aorta taken for Trichrome staining were used. These paraffin-embedded sections (8 micron) were cut, dewaxed, and taken through a standard protocol using a Rabbit Vector kit (Vector Laboratories, Burlingame, CA, USA). Tissue sections were incubated 24 hours with primary antibody against Thrombospondin1 (1:40, Cat # 18304-1-AP, Anti-rabbit). Sections of the superior vena cava were used as a positive control. The same concentration of primary and secondary antibody was used on positive control/aortic/vena cava

sections. Sections were developed according to manufacturer's instructions using a DAB developing solution (Vector Laboratories, Burlingame, CA, USA) for one minute. Binding was observed as a dark brown/black precipitate. All slides were counterstained with Vector Hematoxylin for 20 seconds, with nuclei stained blue. Sections were dried, coverslipped and photographed on a Nikon TE2000 inverted microscope using MetaMorph® software. Autowhite balance was used for all images. When brightness/contrast of these brightfield images were taken, they were done to the whole image and similarly between the images with and without the primary antibody.

Data Presentation

Weights and blood pressures of rats are reported as the means ± SEM for the N=5 for each group. Histological images shown are those originally taken microscopically or brightened/contrasted comparatively between the control and HF condition. Images were brightened/contrasted on the whole, never in part. One RT^2 Profiler Array plate containing a sample of adventitia from a high-fat fed rat did not amplify and was not included in subsequent analyses, meaning that the HF adventitia samples represent an N=4 while all other samples represent N=5. The volcano plot presents the average of the log base 2-fold-change in HF/control in all five pairs on x-axis with log base 10 of the p value generated within the RT^2 Profiler Array Excel file are on the y-axis. Genes 2-fold upregulated at both the 8 and 24 week time point in PVAT and adventitia are shown as color plots, bar scaled for fold change. Cytoscape generated the gene regulatory plots for transcription factors involved in regulating gene sets, again using the mean values for the HF/Con value for all five pairs.

Statistical Analyses

A one-way ANOVA followed by a Sidak's multiple comparison was used to determine statistical differences between the 8 and 24 week weights and the 8 and 24 week blood pressures. Here, a p value of 0.05 or less was considered significant. Analysis of the RT2 Profiler PCR Array results were complete using an Excel template distributed by Qiagen. A Student's t-test was used to calculate the p-values for of the replicate 2-DCT values for each gene in the Profiler Array for adventitia and PVAT at 8 weeks.

RESULTS

Blood pressure and body weights of experimental rats at 8 and 24 weeks on diets

Figure 1 shares the final weights (**Fig. 1a**) and mean arterial blood pressures (MABP; **Fig. 1b)** of animals after 8 and 24 weeks of being on Control or HF diet. The body mass of both Control and HF diet fed rats were greater at 24 weeks compared to their 8-week counterpart group. Moreover, the mass of the HF rat was greater than the Control at the 24 week but not the 8 week time. Similarly, the MABP of the 24 week HF diet fed rat was significantly greater than the paired Control diet fed rat. This was not the case at the 8 week time point in which the blood pressures were statistically similar ($p = 0.082$, Sidak's multiple comparison test). Thus, aortic samples came from animals without (8 week) and with (24 week) elevated mass and blood pressure.

Histology of the thoracic aorta from rats on Control or HF diet for 8 and 24 weeks

The small ring of thoracic aorta that gave rise to the adventitia and PVAT samples used in the RT^2 Profiler Array were saved for histology. **Figure 2** shares the Masson Trichrome staining of an exemplar of each of the five pairs. Of specific importance are the two (2) tunica that were dissected for measure of ECM genes. First, the adventitia stained a brilliant blue, indicative of collagen, in the aorta from animals 8 weeks on diet. Adventitia became more diffuse and less brilliant/dense with age (24 weeks on diet). This staining was more vivid in the adventitia *vs* the PVAT at both 8 and 24 weeks of diet. Second, PVAT was composed primarily of fascia with densely packed/small brown adipocytes in the Control fed rat. Comparatively, the HF diet increased the size and placement of white adipocytes within brown pads. This was readily apparent in the aorta from the rat on the HF diet for 24 weeks. Moreover, collagen was clearly present in the PVAT of the Control and PVAT from the HF rats but less dense than in the adventitia.

Comparison of PVAT to adventitial genes at 8- and 24-weeks of Control or HF diet

The absolute and relative levels of expression of all genes and their associated p values are shared in **Table 1**. At the 8 week time point, changes in the adventitia far outnumbered those observed in PVAT. Specifically, no genes reached the 2-fold threshold for change in the PVAT while 29 did so in the adventitia of the same vessel. **Figure 3a** details these genes in volcano plot form with the top genes that changed to the greatest magnitude labelled. Thrombospondin1 (*Thbs1*) and collagen 8a1 (*Col8a1*) were the genes with the greatest magnitude of change in the

adventitia at this 8 week on diet time point.

By contrast, PVAT had the greatest number of changes at the 24 week time point: 47 genes upregulated 2-fold *vs* the 3 observed in the adventitia (**Fig. 3a**). Here, too, the thrombospondin 1 gene *Thbs1* was one of the top three most upregulated genes. It was accompanied by ADAM metallopeptidase with thrombospondin type 1 motif, 2 (*Adamts2*) and platelet/endothelial cell adhesion molecule 1 (*PECAM1*). **Figure 4** depicts the relative magnitude of changes of gene transcription at the 8 (**Fig. 4a**) and 24 (**Fig. 4b**) week time point. Only the adventitial results are represented in figure 4a because of the lack of genes that changed over 2-fold in PVAT at the 8 week time point. **Figure 6** depicts the significant staining for thrombospondin-1 protein in the adventitia and PVAT at the 8 week and 24 week time points.

Transcriptional drivers of adventitial and PVAT gene changes

The Cystoscape plugin iRegulon allows for tracking of gene changes to curated relationships with transcription factors. **Figure 5** shares these results. For twenty-two (22) of the genes 2-fold upregulated in the adventitia from the 8 week HF fed Dahl SS rat, the transcription factors Adarb1, Fos, Gm10323, Smad3, E2f1, Bcl11a, Rreb1, Jazf1, and MAPK1 were identified. For thirty-five (35) of the genes 2-fold upregulated in the PVAT from the 24 week HF fed Dahl SS rat, Adarb1 was again identified as a potential transcription factor as well as Stat1, Bcl6b, Tsnax, Pax8 and Jun.

DISCUSSION

This study was designed to test the hypothesis that PVAT is responsive to hypertension and likely remodels to assist the blood vessel in protection against higher pressures. We investigated both the PVAT and tunica adventitia of the thoracic aorta. This was done to compare directly how neighboring tissues respond to high fat diet (HFD)-induced hypertension through changes in expression of ECM-related genes, as well as compare PVAT to a tissue better understood in its remodeling in response to hypertension.

Tissue remodeling occurs before and after hypertension

Our data support that ECM remodeling occurs in the thoracic aortic adventitia of the Dahl SS male rat *prior* to the onset of hypertension, and in the PVAT *after* hypertension is established. This general finding is important because it supports the idea that PVAT may be significantly responsive to elevation of blood pressures as opposed to a change in diet. Similarly, the adventitia may be an exquisitely sensitive barometer of local environmental change while PVAT might restrain/retard overall vascular remodeling.

Collagen genes are upregulated in both adventitia and PVAT, but at different times

Collagen is a protein well recognized to be involved in tissue remodeling. The genes for several collagen isoforms changed notably. Specifically, the gene for collagen isoform 4a2, important to the basement membrane of the cell, was upregulated in the adventitia at 8 weeks. *Col2a1*, a fibrillar collagen (Bella & Hulmes, 2017), was upregulated with the HF diet in both tissues, but at different times. It was upregulated at 8 weeks of diet in the adventitia but at 24 weeks in PVAT. Finally, *Col8a1*, the gene for the non-fibrillar short chain collagen, was the most upregulated gene in the adventitia at 8 weeks and upregulated in the PVAT at 24 weeks (Shuttleworth, 1997). This finding is consistent with the upregulation of type 8 (VIII) collagen in diseases or injury involving vascular remodeling (Hansen et al., 2016, Lopes et al., 2013). Upregulation of *Col8a1* during the early remodeling response in the adventitia highlights the sensitivity of this vascular layer. The adventitia may preemptively adapt its ECM to meet changes in diet or before the onset of hypertension. The finding that the adventitia did not exhibit significant further changes at the 24 weeks of diet (comparing HF to Control) while PVAT had marked changes to gene expression is consistent with the idea that remodeling may be complete in the adventitia at this time.

Thrombospondin-1 is upregulated in adventitia and PVAT

The gene *Thbs1*, which encodes for the matricellular ECM protein thrombospondin-1 (TSP1) (Bornstein, 1995), was one of the most upregulated genes in the adventitia at 8 weeks, and PVAT at 24 weeks on HF diet. Indeed, TSP1 staining was significantly higher in the adventitia and PVAT *vs* the media regardless of diet or time point (**Figure 6**). Immunohistochemical staining, considered a qualitative measure, was carried out not to determine whether TSP1 staining became higher in magnitude in PVAT at 24 weeks after the HF *vs* the control diet, but rather to provide evidence that the change in *Thbs1* gene expression was relevant because these tissues ultimately make TSP1.

TSP1 is a regulator of diverse cellular processes. These include ECM organization, matrix metalloproteinase activity, cell adhesion and migration, and apoptosis to name a few (Murphy-Ullrich, 2019). TSP1 also regulates the cellular functions implicated in the ECM homeostasis that are disturbed in remodeling. More specifically, TSP1 regulates the TGF-β pathway by binding and activating latent TGF-β, where activated TGF- β increased myofibroblast differentiation, recruited inflammatory cells, stimulated new matrix deposition, and promoted angiogenesis (Zhang et al., 2020, Rosini et al., 2018, Schultz-Cherry, et al., 1995, Kellouche et al., 2007, Murphy-Ullrich & Poczatek, 2000, Schultz-Cherry et al., 1994). In addition, fibroblast homeostasis is regulated through the C-terminal domain of TSP1 binding to collagen 1 (Rosini et al., 2018). The upregulation of TSP-1 in the adventitia and PVAT supports that both are remodeling their ECM at different times, but through at least one similar pathway. Interference with this pathway would thus potentially reduce remodeling of both layers.

Identifying potential drivers of gene changes in adventitia and PVAT during remodeling

Identification of transcription factors and their respective gene network gives mechanistic insight into what drives disease progression. Using the DEGs (>2FC) of the adventitia and PVAT, a gene regulatory network was computed to identify potential upstream regulators responsible for the observed remodeling in the present study. *Adarb1* (adenosine deaminase RNA specific B1) was the only transcription factor predicted to influence gene expression in both the adventitia at 8 weeks (6 target genes) and PVAT at 24 weeks (12 target genes). Interestingly, the genes *Ncam2*, *Ctnna2*, *Syt1*, *Hapln1*, and *Col8a1* were identified as targets for *Adarb1* in both tissues, but at different times. *Adarb1* was not, however, connected to *Thbs1* in either the adventitia or PVAT. Nonetheless, *Adarb1* may be responsible for mediating the ECM

remodeling responses of both tissue types in this model, potentially identifying a target to ameliorate the observed changes.

PVAT is biologically responsive to hypertension

The present study supports that the thoracic aortic PVAT, a unique fat depot surrounding the vasculature, is sensitive to changes in blood pressure and responds through differential expression of ECM-related genes and in morphology. This finding is consistent with our hypothesis that PVAT remodels its ECM in response to an elevated (sustained) pressure. Here, remodeling may serve as an adaptive response during hypertension to protect the vasculature it surrounds. The impact of this remodeling would be reflected by increased arterial stiffness. PVAT, in a healthy aorta, *reduces* the overall stiffness of the aorta (Tuttle et al., 2022). PVAT itself has a measurably lower stiffness than the artery it surrounds. Collagen content of PVAT was linearly and positively correlated with the low-stress stiffness of the tissue (Tuttle et al., 2022). PVAT might restrain the overall remodeling of the vessel, though unavoidably remodeling itself in the face of persistently elevated blood pressure. To this point, the PVAT of the isolated thoracic aorta of the HF *vs* Con diet fed male Dahl SS rats lost the ability to assist in arterial stress relaxation and displayed a modest increase in PVAT fibrosis (Watts et al., 2021).

Limitations

We recognize limitations to the present study. First, only male Dahl SS rats were used in the current study. In future studies, examining the response of female rats to HF diet induced hypertension in the present context is crucial. Second, study of the media was omitted in this study. Another limitation is that samples from HF or Control animals were only collected at week 8 (before hypertension onset) and 24 (after hypertension onset) for analysis. Other time points may lend insight into the progression of the ECM remodeling. The RT^2 Profiler Array Kit that was used to determine gene expression has the innate limitation of being a finite, curated set of 84 genes related to the ECM. Those genes, however, are well curated and meaningful to the hypothesis at hand. We acknowledge the lack of statistical significance in the DEGs from Control to HF diet animals in both tissue types and timepoints. Despite having a relatively low number of genes reaching statistical significance, the magnitude of genes that had FC >2 at both timepoints may support that there are overall cumulative changes in the gene expression that could harmoniously contribute to ECM remodeling in the face of elevated blood pressure.

While we discuss PVAT and adventitia as independent tunica, growing evidence

strengthens the existence of communication between PVAT and adventitia. For example, the PVAT-derived secretory protein complement 3 induced adventitial fibroblast migration and differentiation to contribute to the adventitial thickening and remodeling in the deoxycorticosterone acetate-salt hypertensive rat model (Ruan et al., 2010). Similarly, adventitial remodeling was promoted by dysfunctional PVAT in the obese mini pig model through the nod-like receptor protein 3 (NLRP3)/Interleukin-1 pathway (Zhu et al., 2019). Communication may occur/mediators may be passed between adventitia and PVAT during onset of hypertension that could mediate the changes in ECM gene expression that were observed in the current study. Tunica cross talk is not something we could measure in this specific study.

CONCLUSIONS

PVAT of the thoracic aorta remodeled its extracellular matrix as a response to elevated blood pressure but not directly to diet. PVAT did not demonstrate biologically relevant changes in ECM genes until an elevated blood pressure was established. This contrasted with the remodeling of the adventitia evident after 8-weeks on the HF diet without an elevation in pressure. The gene *Thbs1* was identified as elevated in the HF *vs* Control diet in both the adventitia and PVAT though at different time points. Collectively, these findings strengthen the foundation that PVAT is a functionally important layer of the blood vessel in sensing and responding to mechanical challenges.

REFERENCES

Humphrey JD. Mechanisms of vascular remodeling in Hypertension. Am J Hypertens. 2021;34(5):432-441.

Majesky MW, Weiser-Evans MCM. The adventitia in arterial development, remodeling, and hypertension. Biochem Pharmacol. 2022;205:115259.

Majesky MW, Dong XR, Hoglund V, Daum G, Mahoney WM. The adventitia: a progenitor cell niche for the vessel wall. Cells Tissues Organs. 2012;195(1-2):73-81.

Michel J-B, Thaunat O, Houard X, Meilhac O, Caligiuri G, Nicoletti A. Topological determinants and consequences of adventitial responses to arterial wall injury. Cells. 2021;10(5):1000.

McGrath JC, Deighan C, Biornes AM, Shafaroudi MM, McBride M, Adler J et al. New aspects of vascular remodelling: the invovlement of all vascular types. Exp Physiology. 2005; 90(4):469-475.

Siow RCM, Churchman AT. Adventitial growth factor signaling and vascular remodeling: potential of perivascular gene transfer from the outside-in. Cardiovasc Res. 2007;75(4) 659-668.

Coen M, Gabbiana G, Bochaton-Piallat M-L. Myofibroblast-mediated adventitial remodeling: an underestimated player in arterial pathology. Arterioscler Thomb Vasc Biol. 2011; 31(11):2391-2396.

Xia N, Li H. The role of perivascular adipose tissue in obesity-induced vascular dysfunction. Br J Pharmacol 2017;174(20):3425-3442.

Gollasch M. Adipose-vascular coupling and potential therapeutics. Annual Rev Pharmacol Toxicol 2017;Jan 6:417-436.

Watts SW, Darios ES, Contreras GA, Garver H, Fink GD. Male and female high-fat diet-fed Dahl SS rats are largely protected from vascular dysfunctions: PVAT contributions reveal sex differences. Am J Physiol Heart Circ Physiol. 2021;321(1):H15-H28.

Beyer AM, Raffai G, Weinberg B, Fredrich K and Lombard JH Dahl salt-sensitive rats are protected against vascular defects related to diet-induced obesity. Hypertension. 2012;60:404-410.

Fernandes R, Garver H, Harkema JR, Galligan JJ, Fink GD and Xu H. Sex differences in renal inflammation and injury in high –fat diet fed Dahl Salt-sensitive rats. Hypertension. 2018;72:e43-e52.

Shannon P, Markiel A, Ozier O, Baliga NS, Wang JT, Ramage D, Amin N, Schwikowski B, Ideker T. Cytoscape: a software environment for integrated models of biomolecular interaction networks. Genome Res. 2003;13(11):2498-504.

Janky R, Verfaillie A, Imrichová H, Van de Sande B, Standaert L, Christiaens V, et al. iRegulon: From a Gene List to a Gene Regulatory Network Using Large Motif and Track Collections. PLoS Comput Biol. 2014;10(7): e1003731.

Bella J, Hulmes DJ. Fibrillar collagens. Subcell Biochem. 2017; 82: 457- 490.

C.A. Shuttleworth. Type VIII collagen. Int J Biochem Cell Biol. 1997;(29):1145-1148

Hansen NU, Willumsen N, Sand JM, Larsen L, Karsdal MA, Leeming DJ. Type VIII collagen is elevated in diseases associated with angiogenesis and vascular remodeling. Clin Biochem. 2016;49(12):903-8.

Lopes J, Adiguzel E, Gu S, Liu SL, Hou G, Heximer S, Assoian RK, Bendeck MP. Type VIII collagen mediates vessel wall remodeling after arterial injury and fibrous cap formation in atherosclerosis. Am J Pathol. 2013;182(6):2241-53.

Bornstein P. Diversity of function is inherent in matricellular proteins: an appraisal of thrombospondin 1. J Cell Biol. 1995;130(3):503–6.

Murphy-Ullrich JE. Thrombospondin 1 and Its Diverse Roles as a Regulator of Extracellular Matrix in Fibrotic Disease. J Histochem Cytochem. 2019;67(9):683-699.

Zhang K, Li M, Yin L, Fu G, Liu Z. Role of thrombosponin-1 and thrombosponin-2 in cardiovascular diseases (review). Int J Mol Med. 2020 45(5):1275-1293.

Rosini S, Pugh N, Bonna AM, Hulmes DJS, Farndale RW, Adams JC. Thrombospondin-1 promotes matrix homeostasis by interacting with collagen and lysyl oxidase precursors and collagen cross-linking sites. Sci Signal. 2018;11(532):eaar2566.

Schultz-Cherry S, Chen H, Mosher DF, Misenheimer TM, Krutzsch HC, Roberts DD, Murphy-Ullrich JE. Regulation of transforming growth factor-beta activation by discrete sequences of thrombospondin 1. J Biol Chem. 1995;270:7304–7310.

Kellouche S, Mourah S, Bonnefoy A, Schoëvaert D, Podgorniak MP, Calvo F, Hoylaerts MF, Legrand C, Dosquet C. Platelets, thrombospondin-1 and human dermal fibroblasts cooperate for stimulation of endothelial cell tubulogenesis through VEGF and PAI-1 regulation. Exp Cell Res. 2007;313:486–499.

Murphy-Ullrich JE, Poczatek M. Activation of latent TGF-beta by thrombospondin-1: Mechanisms and physiology. Cytokine Growth Factor Rev. 2000;11:59–69.

Schultz-Cherry S, Lawler J, Murphy-Ullrich JE. The type 1 repeats of thrombospondin 1 activate latent transforming growth factor-beta. J Biol Chem. 1994;269:26783–26788.

Tuttle T, Darios E, Watts SW, Roccabianca S. Aortic stiffness is lower when PVAT is included: a novel ex vivo mechanics study. Am J Physiol Heart Circ Physiol .2022;322(6):H1003-H0013.

Ruan CC, Zhu DL, Chen QZ, Chen J, Guo SJ, Li XD, Gao PJ. Perivascular adipose tissue-derived complement 3 is required for adventitial fibroblast functions and adventitial remodeling in deoxycorticosterone acetate-salt hypertensive rats. Arterioscler Thromb Vasc Biol. 2010;30 (12):2568-74.

Zhu X, Zhang H-W, Chen H-N, Deng X-J, Tu Y-X, Jackso AO et al. Perivascular adipose tissue dysfunction aggravates adventitial remodeling in obese mini pigs via NLRP3 inflammasome/IL-1 signalling pathway. Acta Pharmacol Sin. 2019;40(1):46-54.

APPENDIX

a.

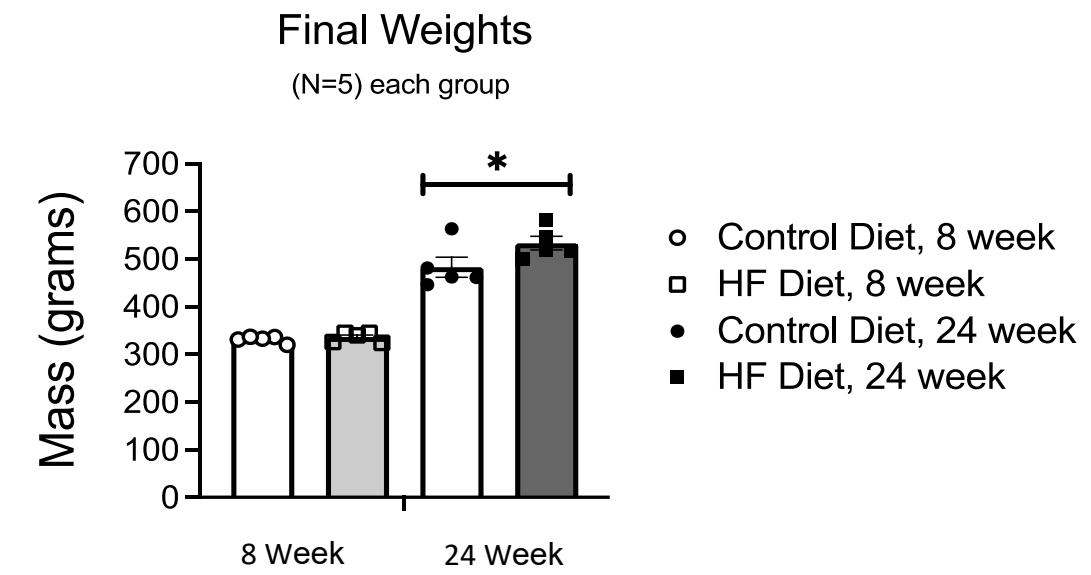

b.

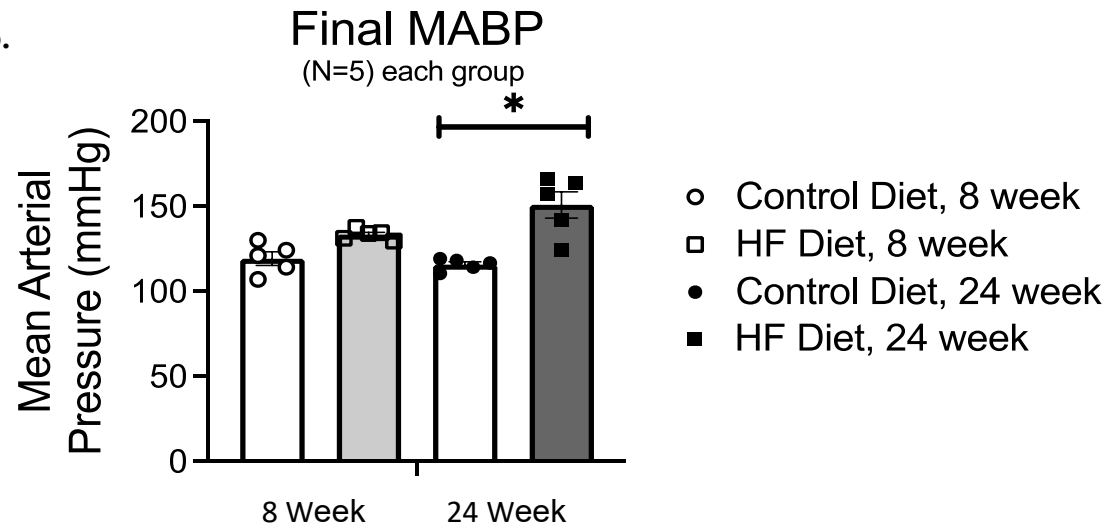

Figure 1. Final body weights and MABP of male Dahl SS rats after 8 or 24 weeks on diet

Final weights of animals (grams) on control or HF diet (a), where the HF diet group had elevated body mass compared to control after 24 weeks on diet. MABP was determined before euthanasia of animals (b), demonstrating that animals after 8 weeks on either diet were normotensive. Animals on 24 weeks of HF diet had statistically elevated blood pressure compared to control. N=5 for all groups. HF=high-fat, MABP=mean arterial blood pressure. *= statistical difference ($p<0.05$) between control and high-fat fed animals.

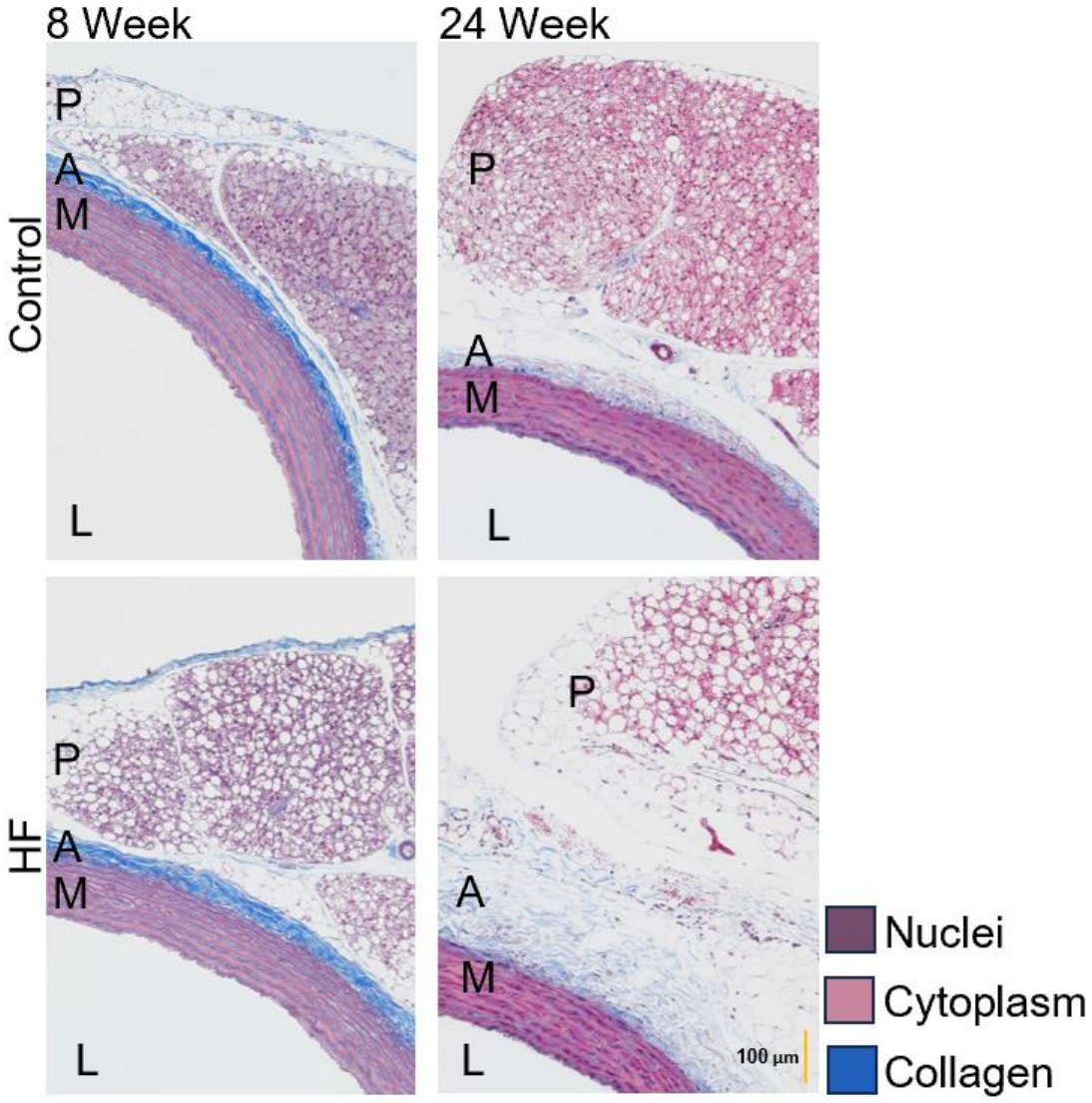

Figure 2. Remodeling of adventitia and PVAT with progression of high-fat diet induced hypertension

Representative images at 10X objective of male Dahl SS rat thoracic aorta and PVAT stained with Masson Trichrome to visualize collagen in blue after 8 (left) or 24 weeks (right) on either control (top) or high-fat (bottom) diet. (Scale bar=100µm) P=perivascular adipose tissue, A=tunica adventitia, M=tunica media, L=lumen.

a.

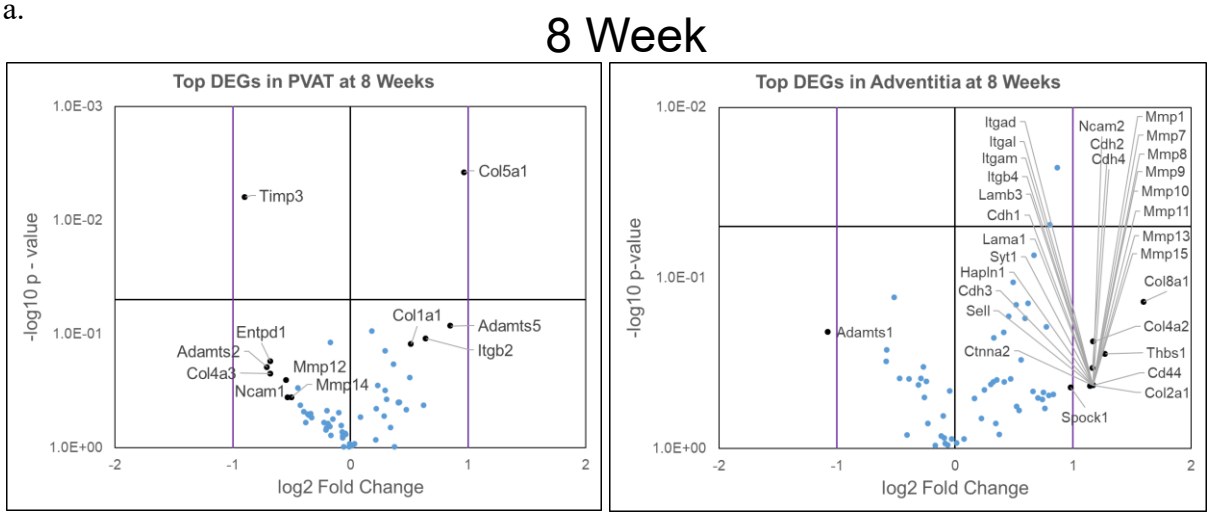

b.

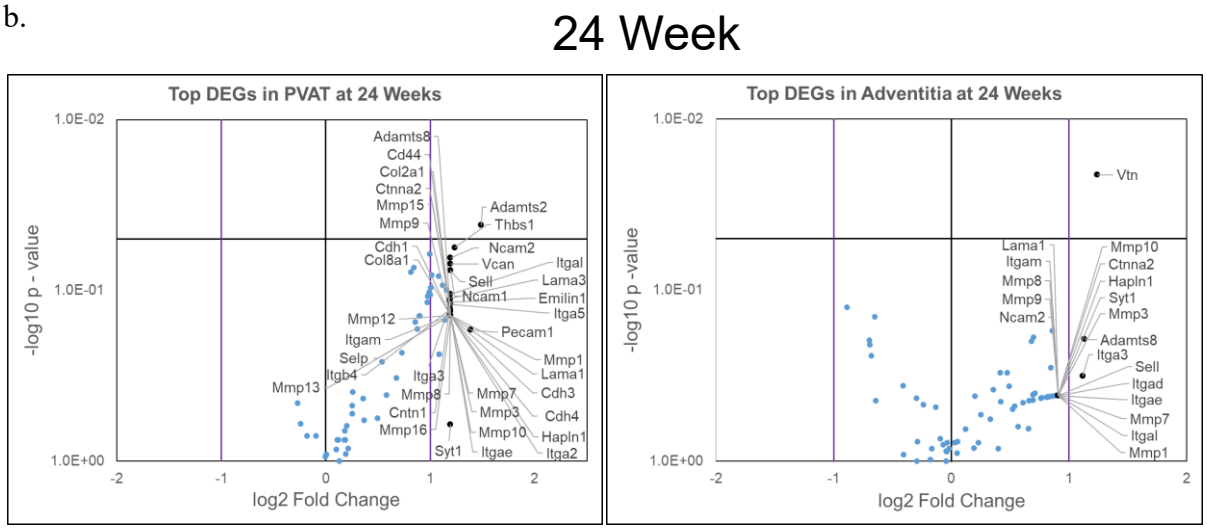

Figure 3. Visualization of results of RT^2 Profiler Array with Volcano Plots

Volcano plots depicting the differential expression of ECM-related genes in thoracic aortic PVAT and adventitia of male Dahl SS rats fed a HF diet. Black line represents a p-value of 0.05, any points above the line having p-value < 0.05 and below a p-value > 0.05. Purple lines representing fold-change or the magnitude of change from control to HF diet animal gene expression. N=5 for all PVAT groups. N=5 for Control adventitia group, N=5 for HF adventitia at 8 weeks, and N=4 for HF adventitia group at 24 weeks.

a.

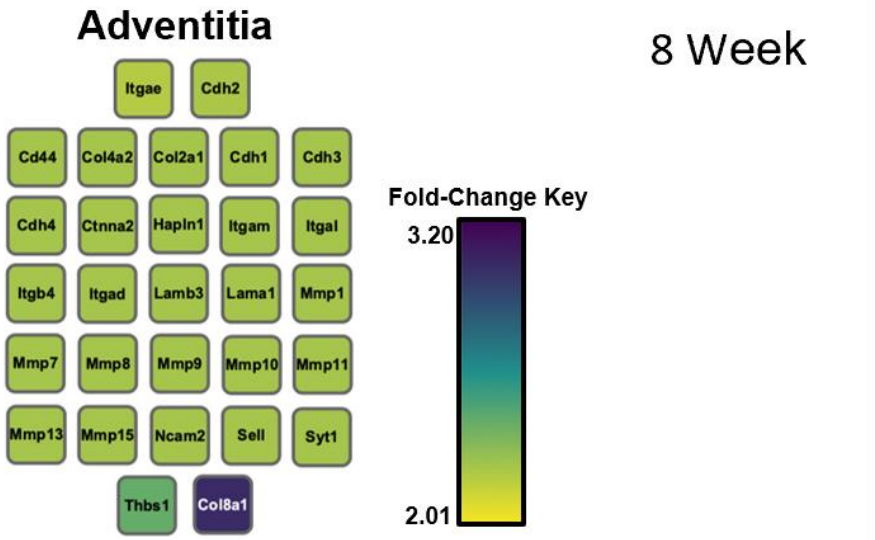

b.

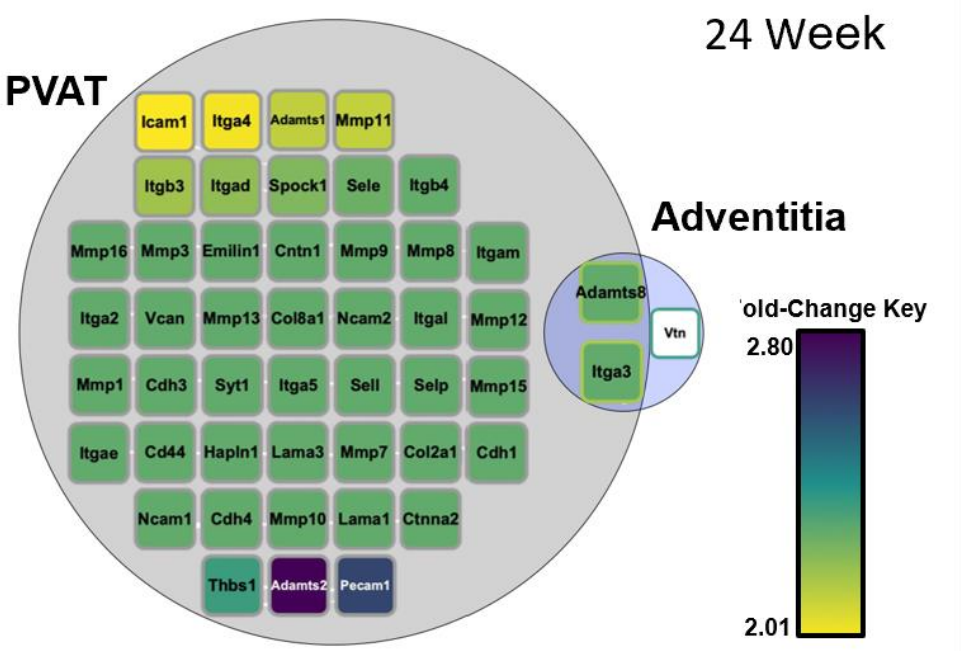

Figure 4. Visualization of results of RT^2 Profiler Array with color plots

Fold-change for each DEG is visualized using Cytoscape through the utilization of color to represent fold-change. After 8 weeks on HFD there were 29 genes with FC>2 in the adventitia and no DEGs in PVAT (a), where shape fill color is representative of FC. A Quantitative Venn Diagram (b) depicting DEGs of ECM-associated genes from control to high-fat diet after 24-week HFD in thoracic PVAT (47 genes) and adventitia (3 genes) tissues. Fold-change for PVAT is represented as shape fill color, while adventitia fold-change is represented as border color. N=5 for all PVAT groups. N=5 for Control adventitia group, N=5 for HF adventitia at 8 weeks, and N=4 for HF adventitia group at 24 weeks.

a.

8 Week Adventitial Transcriptional Drivers

Transcription Factor	Number of Targets	NES
Adarb1	6	6.290
Fos	13	5.161
Gm10323	7	4.755
Smad3	16	4.390
Mapk1	8	4.348
E2f1	9	4.710
Bcl11a	16	4.290
Rreb1	3	4.088
Jazf1	7	4.048

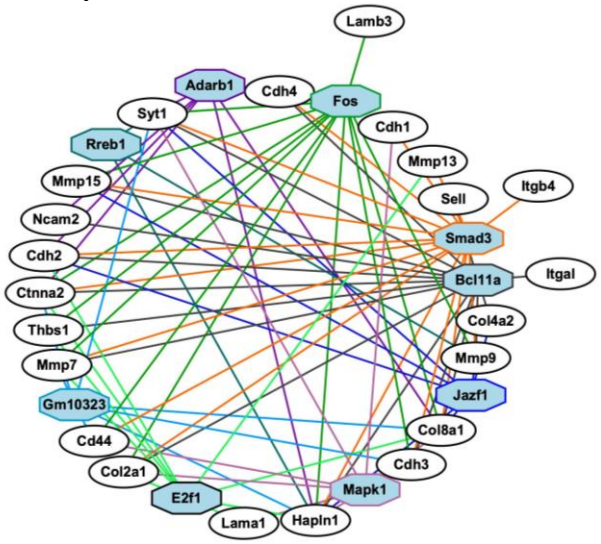

b.

24 Week PVAT Transcriptional Drivers

Transcription Factor	Number of Targets	NES
Stat1	23	5.638
Bcl6b	18	4.575
Tsnax	16	4.493
Adarb1	12	4.485
Pax8	22	4.424
Jun	22	4.174

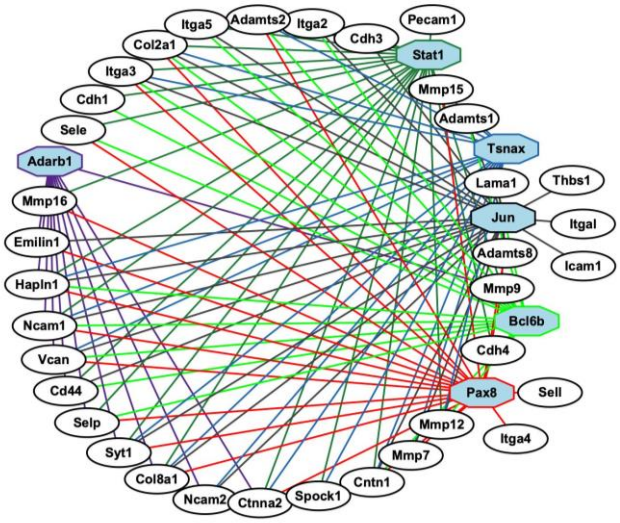

Figure 5. Gene regulatory network may identify transcription factors responsible for remodeling

The Cytoscape plugin iRegulon was used to predict regulatory TFs and construct a gene regulatory network. TFs were included in the analysis with NES >4. TFs are identified by light blue shape fill and a shape outline color matching arrow color. Arrows are directed from TFs to their respective predicted target. The gene regulatory network of the DEGs of the adventitia at 8 weeks (a) predicted 8 TFs regulating 22 out of 29 DEGs. In the DEGs of PVAT at 24 weeks (b), 35 genes out of 47 were predicted to be regulated by 6 TFs. The TF Adarb1 was identified in both gene regulatory networks. N=5 for all PVAT groups. N=5 for Control adventitia group, N=5 for HF adventitia at 8 weeks, and N=4 for HF adventitia group at 24 weeks. DEG=Differentially expressed gene, NES=Normalized enrichment score, TF=Transcription factor.

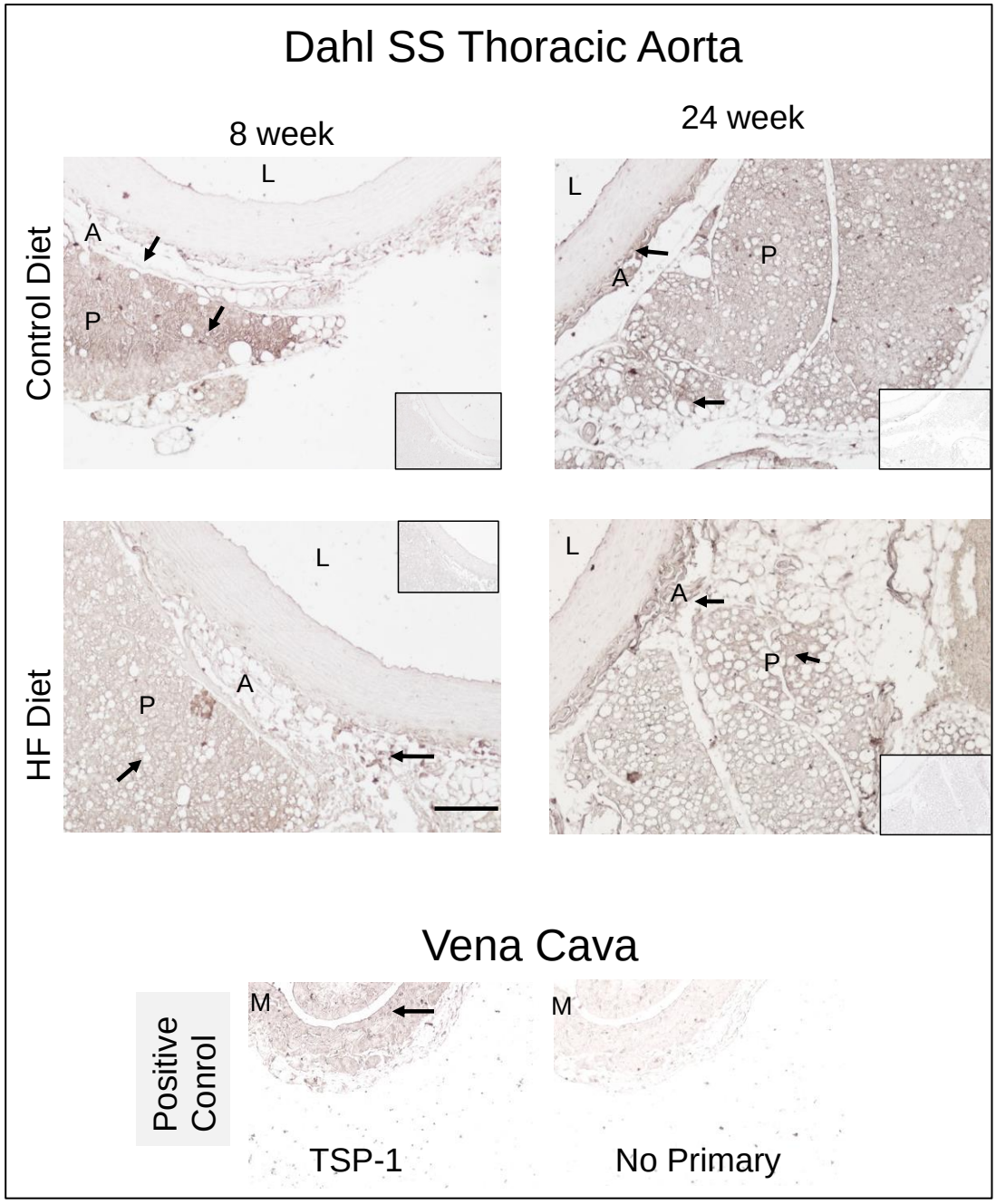

Figure 6. Thrombospondin-1 protein is resident in both the Adventitia and PVAT in the thoracic aorta

Representative images of thrombospondin-1 staining in thoracic aorta + PVAT in the Dahl SS male rat on 8 (left column) or 24 (right column) weeks of either control (top row) or HF (2nd row) of diet. L = lumen, A = adventitia, P = PVAT. The Vena Cava was used as a positive control. Arrows indicate region of interest. Inset box is image of tissue without primary antibody. Representative of four (4) of the 5 groups of rats used in this study. Horizontal bar = 100 micrometers.

Table 1. The absolute and relative levels of expression for ECM-related genes in Adventitia and PVAT after 8 or 24 weeks on diet

		HF/CON				**HF/CON**			
BOLDED = >2 fold change		**8 Week**				**24 Week**			
		Adventitia		**PVAT**		**Adventitia**		**PVAT**	
Gene Abbreviation	**Gene Identification**								
Adamts1	ADAM metallopeptidase with thrombospondin type 1 motif, 1	0.47	0.208551	1.23	0.312363	1.32	0.844702	**2.12**	0.236062
Adamts2	ADAM metallopeptidase with thrombospondin type 1 motif, 2	0.83	0.503743	0.61	0.195847	0.85	0.46775	**2.8**	0.041484
Adamts5	ADAM metallopeptidase with thrombospondin type 1 motif, 5	0.92	0.842989	1.8	0.084772	1.6	0.199426	1.16	0.841614
Adamts8	ADAM metallopeptidase with thrombospondin type 1 motif, 8	1.63	0.505745	0.78	0.514198	**2.19**	0.192675	**2.28**	0.139635
Catna1	Catenin (cadherin associated protein), alpha 1	0.96	0.957035	1.23	0.140012	0.54	0.125818	1.08	0.748871
Cd44	Cd44 molecule	**2.25**	0.426544	0.78	0.506488	1.81	0.416544	**2.28**	0.139635
Cdh1	Cadherin 1	**2.25**	0.426544	0.78	0.514198	1.88	0.4125	**2.28**	0.139635
Cdh2	Cadherin 2	**2.24**	0.338308	1.3	0.980107	1.8	0.283664	**2**	0.106248
Cdh3	Cadherin 3	**2.25**	0.426544	0.78	0.514198	1.88	0.4125	**2.28**	0.139635
Cdh4	Cadherin 4	**2.25**	0.426544	0.78	0.514198	1.88	0.4125	**2.28**	0.139635
Cntn1	Contactin 1	1.27	0.7154	0.86	0.59825	1.45	0.477198	**2.28**	0.116186
Col1a1	Collagen, type I, alpha 1	0.76	0.390571	1.43	0.122342	0.62	0.196201	1.15	0.618375
Col2a1	Collagen, type II, alpha 1	**2.25**	0.426544	0.78	0.514198	1.88	0.4125	**2.28**	0.139635
Col3a1	Collagen, type III, alpha 1	1.25	0.225276	1.17	0.283141	0.62	0.241327	0.88	0.710414
Col4a1	Collagen, type IV, alpha 1	1.01	0.927021	0.89	0.118092	0.82	0.997707	0.83	0.456265
Col4a2	Collagen, type IV, alpha 2	**2.25**	0.236822	0.95	0.780944	1.39	0.303401	1.14	0.907718
Col4a3	Collagen, type IV, alpha 3	1.23	0.421439	0.62	0.222243	1.64	0.40041	1.99	0.102722
Col5a1	Collagen, type V, alpha 1	0.7	0.129678	1.95	0.003787	0.64	0.142817	1.09	0.99898
Col6a1	Collagen, type VI, alpha 1	0.67	0.308425	0.9	0.557095	0.98	0.77797	1.07	0.856192

Table 1 (cont'd)

Col8a1	Collagen, type VIII, alpha 1	**3.03**	0.138332	0.78	0.514198	1.81	0.172648	**2.28**	0.139635
Ctgf	Connective tissue growth factor	1.33	0.408371	0.96	0.980722	1.15	0.41725	1.59	0.324376
Ctnna2	Catenin (cadherin associated protein), alpha 2	**2.25**	0.426544	0.78	0.514198	1.88	0.4125	**2.28**	0.13252
Ctnnb1	Catenin (cadherin associated protein), beta 1	1.25	0.408053	1.32	0.396422	0.97	0.871093	0.85	0.605243
Ecm1	Extracellular matrix protein 1	1.05	0.879192	0.95	0.721547	0.91	0.483367	1.81	0.15331
Emilin1	Elastin microfibril interfacer 1	1.78	0.480747	0.78	0.514198	0.97	0.999962	**2.28**	0.117117
Entpd1	Ectonucleoside triphosphate diphosphohydrolase 1	0.89	0.961393	0.62	0.173615	1.03	0.895562	2	0.061025
Fbln1	Fibulin 1	0.72	0.3879	0.99	0.92065	0.62	0.207833	1.45	0.261916
Fn1	Fibronectin 1	1.17	0.666907	1.22	0.52408	0.75	0.916293	1.13	0.662841
Hapln1	Hyaluronan and proteoglycan link protein 1	**2.25**	0.426544	0.78	0.514198	1.88	0.4125	**2.28**	0.139635
Icam1	Intercellular adhesion molecule 1	1.59	0.073663	1.33	0.395443	1.57	0.64529	**2.01**	0.096517
Itga2	Integrin, alpha 2	1.46	0.598119	0.97	0.762536	1.88	0.4125	**2.28**	0.139635
Itga3	Integrin, alpha 3	1.73	0.490205	0.89	0.774434	**2.17**	0.318011	**2.28**	0.118575
Itga4	Integrin, alpha 4	1.7	0.582493	0.87	0.66432	1.88	0.4125	**2.02**	0.081293
Itga5	Integrin, alpha 5 (fibronectin receptor, alpha polypeptide)	1.44	0.566926	0.78	0.514198	1.62	0.40785	**2.28**	0.120666
Itgad	Integrin, alpha D	**2.25**	0.426544	1.39	0.460784	1.88	0.4125	**2.2**	0.149405
Itgae	Integrin, alpha E	**2.21**	0.430728	0.78	0.514198	1.88	0.4125	**2.28**	0.139635
Itgal	Integrin, alpha L	**2.25**	0.426544	0.95	0.812148	1.88	0.4125	**2.28**	0.104941
Itgam	Integrin, alpha M	**2.25**	0.426544	0.78	0.514198	1.88	0.4125	**2.28**	0.139635
Itgav	Integrin, alpha V	1.54	0.141375	1.24	0.372944	0.99	0.842516	1.09	0.752366
Itgb1	Integrin, beta 1	1.37	0.167628	0.93	0.491594	0.82	0.767487	1.19	0.472856
Itgb2	Integrin, beta 2	0.82	0.389657	1.56	0.109204	1.58	0.442458	1.79	0.073685
Itgb3	Integrin, beta 3	1.58	0.462275	0.78	0.514198	1.43	0.494551	**2.17**	0.092941
Itgb4	Integrin, beta 4	**2.25**	0.426544	0.78	0.514198	1.75	0.420651	**2.28**	0.128987
Lama1	Laminin, alpha 1	**2.25**	0.426544	0.78	0.514198	1.88	0.4125	**2.28**	0.139635
Lama2	Laminin, alpha 2	1.33	0.208304	1	0.938021	0.94	0.735998	1.28	0.430791
Lama3	Laminin, alpha 3	1.3	0.825973	0.8	0.543069	1.48	0.625865	**2.28**	0.111303
Lamb2	Laminin, beta 2	1.43	0.144247	0.95	0.6352	0.89	0.84472	1.49	0.410013
Lamb3	Laminin, beta 3	**2.25**	0.426544	0.78	0.514198	1.71	0.425105	1.83	0.168345
Lamc1	Laminin, gamma 1	0.85	0.405646	1.01	0.956764	1.28	0.380409	1	0.937069

Table 1 (cont'd)

Mmp10	Matrix metallopeptidase 10	**2.25**	0.426544	0.78	0.514198	1.88	0.4125	**2.28**	0.139635
Mmp11	Matrix metallopeptidase 11	**2.25**	0.426544	0.86	0.696912	1.61	0.438479	**2.11**	0.082244
Mmp12	Matrix metallopeptidase 12	0.97	0.460524	0.68	0.254984	1.53	0.45404	**2.28**	0.139635
Mmp13	Matrix metallopeptidase 13	**2.25**	0.426544	0.76	0.482177	1.88	0.4125	**2.28**	0.139635
Mmp14	Matrix metallopeptidase 14 (membrane-inserted)	1.28	0.395715	0.71	0.359091	1.02	0.779647	1.76	0.07832
Mmp15	Matrix metallopeptidase 15	**2.25**	0.426544	0.78	0.514198	1.88	0.4125	**2.28**	0.131325
Mmp16	Matrix metallopeptidase 16	1.68	0.469895	0.78	0.514198	1.84	0.414523	**2.28**	0.139635
Mmp1	Matrix metallopeptidase 1a (interstitial collagenase)	**2.25**	0.426544	0.78	0.514198	1.88	0.4125	**2.28**	0.139635
Mmp2	Matrix metallopeptidase 2	1.12	0.507937	0.73	0.296872	0.75	0.361293	1.13	0.750811
Mmp3	Matrix metallopeptidase 3	0.67	0.264197	0.78	0.514198	1.88	0.4125	**2.28**	0.139635
Mmp7	Matrix metallopeptidase 7	**2.25**	0.426544	0.78	0.514198	1.88	0.4125	**2.28**	0.139635
Mmp8	Matrix metallopeptidase 8	**2.25**	0.426544	0.78	0.514198	1.88	0.4125	**2.28**	0.139635
Mmp9	Matrix metallopeptidase 9	**2.25**	0.426544	0.78	0.514198	1.88	0.4125	**2.28**	0.139635
Ncam1	Neural cell adhesion molecule 1	1.75	0.04871	0.69	0.361512	1.26	0.568614	**2.28**	0.075813
Ncam2	Neural cell adhesion molecule 2	**2.25**	0.426544	0.89	0.650328	1.88	0.4125	**2.28**	0.064482
Pecam1	Platelet/endothelial cell adhesion molecule 1	1.51	0.172947	1.54	0.419521	1.62	0.188309	**2.62**	0.170147
Postn	Periostin, osteoblast specific factor	1.71	0.193679	1.13	0.094298	0.97	0.880192	1.29	0.577475
Sele	Selectin E	0.93	0.643118	0.79	0.500679	1.34	0.447935	**2.27**	0.115479
Sell	Selectin L	**2.25**	0.426544	1.16	0.451046	1.88	0.4125	**2.28**	0.076477
Selp	Selectin P	1.67	0.516275	0.78	0.514198	1.77	0.419518	**2.28**	0.139635
Sgce	Sarcoglycan, epsilon	0.83	0.333458	0.99	0.980541	1.33	0.303203	1.41	0.560502
Sparc	Secreted protein, acidic, cysteine-rich (osteonectin)	0.98	0.879272	1.29	0.1833	1.09	0.646491	1.01	0.915467
Spock1	Sparc/osteonectin, cwcv and kazal-like domains proteoglycan (testican) 1	1.97	0.439024	0.97	0.746709	1.77	0.419064	**2.23**	0.098979
Spp1	Secreted phosphoprotein 1	1.19	0.455051	1.32	0.400209	0.64	0.44197	1.87	0.141288

Table 1 (cont'd)

Syt1	Synaptotagmin I	**2.25**	0.426544	0.77	0.600322	1.88	0.4125	**2.28**	0.609659
Tgfbi	Transforming growth factor, beta induced	0.85	0.714402	0.78	0.514198	1.04	0.767841	1.86	0.140801
Thbs1	Thrombospondin 1	**2.42**	0.279098	0.88	0.608742	1.69	0.426543	**2.35**	0.05606
Thbs2	Thrombospondin 2	0.75	0.833778	1.42	0.240028	1.41	0.364759	1.96	0.117764
Timp1	TIMP metallopeptidase inhibitor 1	1.41	0.106101	1.02	0.921845	1.19	0.53468	1.14	0.752701
Timp2	TIMP metallopeptidase inhibitor 2	0.94	0.934397	1.06	0.537585	0.81	0.427482	1.19	0.526528
Timp3	TIMP metallopeptidase inhibitor 3	1.82	0.022644	0.54	0.006269	0.88	0.978859	0.94	0.709963
Tnc	Tenascin C	1.47	0.303013	1.27	0.662127	1.17	0.779541	1.97	0.107988
Vcam1	Vascular cell adhesion molecule 1	1.39	0.391319	0.74	0.422494	0.95	0.799497	1.66	0.232239
Vcan	Versican	0.94	0.868758	0.87	0.470667	1.14	0.838404	**2.28**	0.069843
Vtn	Vitronectin	0.81	0.424098	1.16	0.848173	**2.36**	0.021202	1.2	0.392269